

A Novel Fault Soft Interruption Scheme Suitable for Smart Circuit Breakers

Xiao Ma¹, Xiangning Lin¹, Yuqi Wu¹, Shankang Cao¹, Zhengtian Li¹ and Fanrong Wei¹

¹ State Key Laboratory of Advanced Electromagnetic Engineering and Technology, Huazhong University of Science and Technology, Wuhan, China

Abstract. With the rapid development of smart substations, the application of smart circuit breakers (CB) has acquired a substantial technical basis. One of the key issues is that the short-circuit current (SCC) and arcing duration time in fault interruption have great impacts on the life of CB. To this end, a novel fault soft interruption (FSI) scheme is proposed in this paper. First, a novel phaselet-based estimation algorithm is put forward, utilizing samples in an ultra-short time window, and thus the current zero-crossing points of the coming several cycles can be predicted accurately. Then, the earliest feasible zero-crossing point is determined, by which the CB is controlled to separate its contacts at the favorable instant when SCC descends below the interrupting rating (IR) safely while keeping the arcing time minimized. The simulation testifies the performance of the proposed scheme under various fault scenarios, such as time constants and fault inception angles. The results show that compared with the conventional way, the proposed scheme can prolong the life cycle of CB and cope with the potential excessive SCC risks at relatively less cost.

Keywords: smart circuit breaker, fault interruption, interrupting rating, short-circuit current, online parameter estimation.

1. Introduction

The smart substation is playing an important role in promoting the development of smart grids [1]-[3]. As a key apparatus in the smart substation, the circuit breaker (CB) is responsible for switching currents (closing or opening) to meet various demands of power systems, e.g., fault clearing, optimal transmission switching [4], et al. How to make the CB more “smart” to improve its operating reliability and lengthen its lifetime, which affects the life cycle cost (LCC) of the whole substation, is drawing intense research interests [5].

The most distinguished advantage of the smart CB relies on the controlled switching technology. It can automatically adjust the contact parting instant so that the current would be interrupted at the expected zero-crossing point through the minimum arcing time, thus decreasing the electrical wears greatly [6]. To do so, the first core technological foundation is to adequately shorten the opening time and minimum arcing time of the CB and limit their variations meanwhile. There are a lot of research works in this respect. Especially in recent years, the vacuum CB equipped with the magnetic or electronic mechanism has been extensively studied, for its higher operating accuracy than the conventional gas CB. Ref. [7] utilized the fuzzy self-adaptive approach to make the contacts move following the predetermined route, keeping the operating time dispersion within ± 0.25 ms. Further, a novel fiber-controlled vacuum interrupter module was proposed, which could be combined in series to establish the extra-high-voltage (EHV) vacuum CB [8].

The second essential basis of the controlled switching technology is to predict current waveforms online. A safe-point strategy was proposed by [9], which substituted so-called safe-points for real zero-crossing points, with the time request no longer than a half-cycle. However, since the safe-points always precede the corresponding zero-crossing points, the aforementioned measure is so conservative that it cannot achieve the target of optimizing arcing times. The least means square (LMS) principle was used by [10] to estimate the parameters of short-circuit currents (SCC), but it could not avoid the truncation error caused by the Taylor series expansion of the dc exponential term. The adaptive Prony method [11] was also applied to modeling fault currents, but it was unable to meet the real-time requirement. Some intelligent algorithms have gained popularity in this field as well, such as the artificial neural network (ANN) [12], support vector regression

(SVR) [13], of which the major concern is that they need a lot of data for off-line training. Nevertheless, for the current approaches to estimating SCC parameters, the biggest problem is that it is still pretty hard to complete the work precisely within the protection response time, restricting the practical application of the smart CB in EHV power grids.

Another challenge for the smart CB is the growing scale of SCC in EHV transmission systems, which is one of the serious obstacles facing the East China Grid [14]. Particularly, it is always believed that the dc component has fully decayed (<20%) when the CB is prepared to part its contacts. So the contribution of the dc component to the interrupting pressure has long been neglected. However, as the capacity of inductive equipment surges and the coupling of power systems strengthens, the dc decaying time constant gradually increases, while the protection operating time keeps decreasing because of the novel protective criteria being more and more sensitive. In consequence, there is a rising trend of the residual dc component at the contact separation instant [15], boosting the risk of SCC exceeding the interrupting rating (IR) of the CB. The risk of excessive SCC appears under certain topologies and operation conditions, and it is closely related to fault inception instants. For such a small-probability event, the adoption of traditional means (e.g., equipment upgrading, bus splitting, applying fault current limiters), damages the economy of power systems. By contrast, the controlled switching technology can provide a new opportunity to the above critical issue. Rather than directly interrupt the excessive SCC immediately after receiving the protection tripping signal, it should separate the contacts exactly when the SCC falls below the IR, based on the online estimation results. Therefore, it is hopeful to settle the excessive SCC problem by the smart CB itself, avoiding or postponing the configuration of extra expensive current-limiting devices. However, if not improved specifically, the original controlled switching technology cannot satisfy this emerging demand.

Therefore, in order to make the smart CB in better coordination with protection systems and adapt to the increasing threat of excessive SCC, this paper presents a novel fault soft interruption (FSI) scheme. The contributions are summarized as follows:

- 1) Compared with the general controlled switching technology, the concept of “soft” focuses on the unity of dual purposes, i.e., arcing time minimization, and excessive SCC suppression, to further optimize the performance of the smart CB in fault interruption.

- 2) Utilizing the novel phaselet-based estimation algorithm, the zero-crossing points of SCC can be predicted reliably within 1/4 cycle, ensuring that the proposed scheme can cooperate well with the existing protection relays.

- 3) A comprehensive scheme is put forward, including the evaluation of excessive SCC, together with the aim of minimizing arcing time, seeking the feasible zero-crossing point to trip the CB safely with the least electrical wear.

The rest of this paper is organized as follows: Section II analyzes the potential risks of the conventional interruption mode (a.k.a., fault direct interruption). Section III presents the principle of the fault soft interruption scheme. Section IV verifies the effectiveness of the proposed method. Section V concludes this paper.

2. Potential Risks of the Fault Direct Interruption

Regarding the fault direct interruption (FDI), the trip command is sent to the CB as soon as the corresponding protection operates, as shown in Fig. 1. In this case, the actual arcing time Δt_{arc} might be much longer than the minimum arcing time Δt_{arcmin} (the shortest required time to reach the critical gap between contacts so that the dielectric strength is enough to prevent the arc re-ignition [9]), increasing the contact wear adversely.

To be worse, under some severe faults with large dc decaying time constants especially when occurring exactly at the voltage zero-crossing point (stirring up the greatest dc component magnitude), the total RMS value of SCC at contact separation might exceed the IR of the CB. Once the FDI mode attempts to trip the CB forcibly in such scenarios, there would be a considerable possibility of interruption failure, due to the hazardous effects of excessive mechanical and thermal stresses on the interrupting chamber. Then it has to be remedied by backup protection, e.g., the breaker failure protection [16], [17], which would not only extend

the fault clearing time (FCT) significantly but also trip all the surrounding CB, causing huge danger to the stability and integrity of power systems.

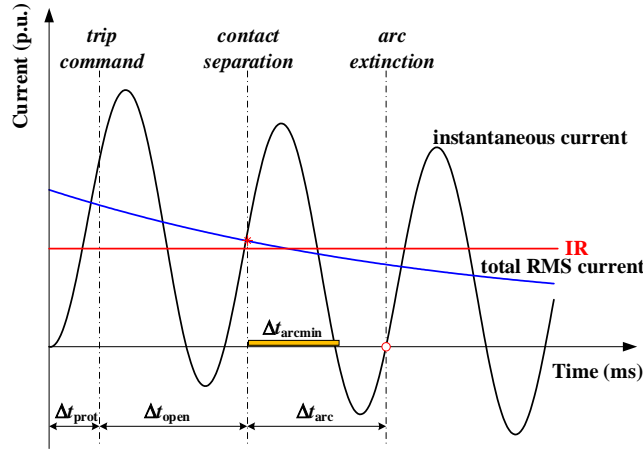


Fig. 1: Process of the fault direct interruption

Thus it can be seen that the fault direct interruption is not the optimal nor safe way to deal with the above challenges. If aided by an appropriate estimation algorithm, it is practical to identify such risks in advance, and then control the CB to be interrupted securely at the predefined instant, which is right the task of the proposed fault soft interruption scheme.

3. Principle of the Fault Soft Interruption

3.1. Ultra-fast SCC parameter estimation

Since the fastest EHV transmission line protection can react around 6 ms [9], the estimation of SCC parameters should be carried out within 1/4 cycle. For most existing algorithms (e.g., LMS, SVR, Prony, et al), it is hard to converge in such an ultra-short time window. Thus, a novel phaselet-based estimation algorithm has been put forward.

Unlike the standard Fourier algorithm using a full-cycle or half-cycle time window, the phaselet algorithm can calculate phasors with the time expenditure of less than a half-cycle [18], [19]. The real part and imaginary part of the n^{th} phaselet P_n ($P_n = [P_{\text{ren}} \ P_{\text{imn}}]^T$) can be expressed as:

$$\begin{cases} P_{\text{ren}} = \sum_{k=(n-1)m+1}^{nm} i(k) \cdot \cos\left(\frac{2\pi k}{N}\right) \\ P_{\text{imn}} = \sum_{k=(n-1)m+1}^{nm} i(k) \cdot \sin\left(\frac{2\pi k}{N}\right) \end{cases} \quad (1)$$

where N is the number of samples per cycle; m is the number of samples per phaselet, i.e., one fundamental cycle is divided into N/m phaselets.

For a pure sinusoidal signal, the fundamental-frequency phasor I_F ($I_F = [I_{F\text{re}} \ I_{F\text{im}}]^T$) can be given by:

$$I_F = T_n \cdot P_n \quad (2)$$

where $T_n = \begin{bmatrix} \sum_{k=(n-1)m+1}^{nm} \cos^2\left(\frac{2\pi k}{N}\right) & \sum_{k=(n-1)m+1}^{nm} \frac{1}{2} \sin\left(\frac{4\pi k}{N}\right) \\ \sum_{k=(n-1)m+1}^{nm} \frac{1}{2} \sin\left(\frac{4\pi k}{N}\right) & \sum_{k=(n-1)m+1}^{nm} \sin^2\left(\frac{2\pi k}{N}\right) \end{bmatrix}^{-1}$ is the transformation matrix which can be precomputed

easily.

Note that the current signal during the fault period usually contains the decaying dc offset, as shown in (3).

$$i(t) = A_0 e^{-\frac{t}{\tau}} + A_1 \sin(\omega t + \theta_1) \quad (3)$$

where A_0 is the magnitude of the dc offset; τ is the time constant of the decaying component; A_1, θ_1 is the amplitude, angle of the fundamental-frequency component respectively.

Sampling the fault current every ΔT , and applying the phaselet algorithm directly, yields:

$$\mathbf{T}_n \cdot \mathbf{P}_n = \mathbf{T}_n \cdot \mathbf{A}_n + \mathbf{I}_F \quad (4)$$

where $\mathbf{A}_n = \begin{bmatrix} \sum_{k=(n-1)m+1}^{nm} A_0 e^{-\frac{k\Delta T}{\tau}} \cdot \cos(\frac{2\pi k}{N}) \\ \sum_{k=(n-1)m+1}^{nm} A_0 e^{-\frac{k\Delta T}{\tau}} \cdot \sin(\frac{2\pi k}{N}) \end{bmatrix}$ represents the error introduced by the dc offset.

It can be seen from (4) that the fundamental-frequency phasor \mathbf{I}_F cannot be obtained solely through (1)-(2) in the case of dc offsets. In other words, the dc offset can have a drastic impact on the calculation of fundamental-frequency phasors utilizing just one phaselet.

To effectively extract both the dc and ac components, one practical way is to differentiate over adjacent phaselets. Obviously, (4) can also apply to the $n+1^{\text{th}}$, $n+2^{\text{th}}$ phaselets, then

$$\begin{cases} \mathbf{T}_{n+1} \cdot \mathbf{P}_{n+1} - \mathbf{T}_n \cdot \mathbf{P}_n = \mathbf{T}_{n+1} \cdot \mathbf{A}_{n+1} - \mathbf{T}_n \cdot \mathbf{A}_n \\ \mathbf{T}_{n+2} \cdot \mathbf{P}_{n+2} - \mathbf{T}_{n+1} \cdot \mathbf{P}_{n+1} = \mathbf{T}_{n+2} \cdot \mathbf{A}_{n+2} - \mathbf{T}_{n+1} \cdot \mathbf{A}_{n+1} \end{cases} \quad (5)$$

Meanwhile, $\mathbf{A}_n, \mathbf{A}_{n+1}, \mathbf{A}_{n+2}$ follow the relationship as below:

$$\begin{cases} \mathbf{A}_{n+1} = E \mathbf{K} \mathbf{A}_n \\ \mathbf{A}_{n+2} = E \mathbf{K} \mathbf{A}_{n+1} \end{cases} \quad (6)$$

where E ($E = e^{-m(\Delta T/\tau)}$) represents the decaying coefficient; $\mathbf{K} = \begin{bmatrix} \cos(\frac{2\pi m}{N}) & -\sin(\frac{2\pi m}{N}) \\ \sin(\frac{2\pi m}{N}) & \cos(\frac{2\pi m}{N}) \end{bmatrix}$ is the association matrix.

Theoretically, combining (5)-(6) can produce a quadratic equation about E , by which the time constant τ can be solved. However, it requires lots of matrix operations to get such an equation, and its coefficients are matrixes but not single numbers. Instead, the method based on dichotomy is not subject to the above problems. Considering that the time constant τ usually ranges above 10 ms in the EHV network, the value of E is between 0.8 and 1.0 when the time window of each phaselet is less than 1/8 cycle. Therefore, the dichotomy solution can be performed as follows:

1) Set the solution interval $[E_{\text{low}}, E_{\text{up}}]$ (initially to be [0.8, 1.0]), and select its midpoint as the estimation, i.e. \hat{E} .

2) Substituting the \hat{E} into (5)-(6) yields:

$$\begin{cases} \hat{\mathbf{A}}_n = (\mathbf{T}_{n+1} \cdot \hat{E} \mathbf{K} - \mathbf{T}_n)^{-1} \cdot (\mathbf{T}_{n+1} \cdot \mathbf{P}_{n+1} - \mathbf{T}_n \cdot \mathbf{P}_n) \\ \hat{\mathbf{A}}_{n+1} = (\mathbf{T}_{n+2} \cdot \hat{E} \mathbf{K} - \mathbf{T}_{n+1})^{-1} \cdot (\mathbf{T}_{n+2} \cdot \mathbf{P}_{n+2} - \mathbf{T}_{n+1} \cdot \mathbf{P}_{n+1}) \end{cases} \quad (7)$$

3) When 1/2 length of the solution interval is already less than the preset error threshold ε , end the process assuming the present estimation ($\hat{E}, \hat{\mathbf{A}}_n$) to be the final solution. Otherwise, continue.

4) According to the estimated $\hat{\mathbf{A}}_n$ and $\hat{\mathbf{A}}_{n+1}$, the decaying coefficient can be recalculated, defined as \hat{E}_{re} , i.e.,

$$\hat{E}_{\text{re}} = (\mathbf{K} \hat{\mathbf{A}}_n)^+ \cdot \hat{\mathbf{A}}_{n+1} \quad (8)$$

where $(\mathbf{K} \hat{\mathbf{A}}_n)^+$ is the left pseudoinverse of $\mathbf{K} \hat{\mathbf{A}}_n$.

5) Compare \hat{E} and \hat{E}_{re} . If $\hat{E} \leq \hat{E}_{\text{re}}$, meaning that the estimated value \hat{E} is still smaller than the actual one E , then replace the solution interval with a new lower bound $E_{\text{low}} = \hat{E}$. Otherwise, update the upper bound E_{up} to be \hat{E} . Repeat the above procedures until the desired accuracy is satisfied.

Based on the final solution obtained by the dichotomy, the ac component of the fault current shown in (3) can be given by:

$$\begin{cases} \hat{\mathbf{I}}_F = [\hat{I}_{Fre} \ \hat{I}_{Fim}]^T = \mathbf{T}_n \cdot \mathbf{P}_n - \mathbf{T}_n \cdot \hat{\mathbf{A}}_n \\ \hat{A}_1 = \sqrt{\hat{I}_{Fre}^2 + \hat{I}_{Fim}^2} \\ \hat{\theta}_1 = \arctan\left(\frac{\hat{I}_{Fre}}{\hat{I}_{Fim}}\right) \\ \hat{i}_{ac}(k) = \hat{A}_1 \sin(\omega \cdot k\Delta T + \hat{\theta}_1) \end{cases} \quad (9)$$

Further, the dc component can be given by:

$$\begin{cases} \hat{A}_0 = \frac{1}{m} \sum_{k=(n-1)m+1}^{nm} [i(k) - \hat{i}_{ac}(k)] \\ \hat{\tau} = -\frac{m\Delta T}{\ln(\hat{E})} \\ \hat{i}_{dc}(k) = \hat{A}_0 \cdot e^{-\frac{k\Delta T}{\hat{\tau}}} \end{cases} \quad (10)$$

Eventually, the instantaneous and total RMS values of the estimated SCC can be calculated as:

$$\hat{i}(k) = \hat{A}_0 \cdot e^{-\frac{k\Delta T}{\hat{\tau}}} + \hat{A}_1 \sin(\omega \cdot k\Delta T + \hat{\theta}_1) \quad (11)$$

$$\hat{I}(k) = \sqrt{(\hat{A}_0 \cdot e^{-\frac{k\Delta T}{\hat{\tau}}})^2 + \frac{\hat{A}_1^2}{2}} \quad (12)$$

In the scope of this paper, utilizing the 1st to 3rd phaselets with the 1/16-cycle time window each after fault initiation for the dichotomy solution, the goal of estimating SCC parameters can be accomplished within 1/4 cycle.

3.2. Search of the feasible current zero-crossing point

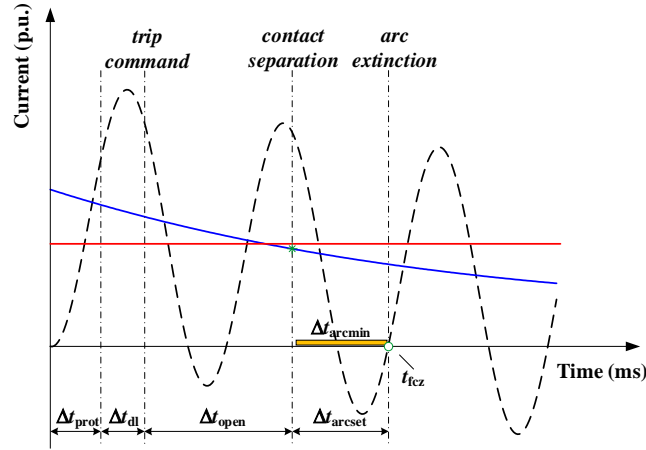


Fig. 2: Search of the feasible current zero-crossing point.

Based on the proposed estimation algorithm, the SCC waveform can be extrapolated to search for the earliest feasible current zero-crossing point t_{fcz} , as shown in Fig. 2.

The first thing to be noted is that the feasible current zero-crossing point should lag a specific period, i.e., the opening time Δt_{open} (the time interval between energization of tripping coils and contact separation [9]) plus the minimum arcing time Δt_{arcmin} , behind the moment of protection operating. The aim is to ensure sufficient contact gap and dielectric buildup for arc-reignition avoidance.

Another focus on the feasible current zero-crossing point is that no excessive SCC at the desired contact separation instant, earlier than the feasible current zero-crossing point by Δt_{arcset} ($\Delta t_{\text{arcset}} = \Delta t_{\text{arcmin}} + \Delta t_{\text{mg}}$, where Δt_{mg} is the safety margin enduring the stochastic scatters of mechanical drive and estimation errors [9]).

Here, in order to evaluate the SCC excessive risk, it is critical to clarify the IR of CB. In IEEE and IEC series standards for CB [20]-[22], the main basis of the IR is the rated symmetrical SCC interrupting capability I_{sym} (the maximum withstanding RMS value of the ac component, considering the dc component of no more than 20% at the instant of contact separation), i.e.,

$$IR = I_{\text{sym}} \cdot \sqrt{1 + 2 \times 0.2^2} \quad (13)$$

In summary, the requirements of the feasible current zero-crossing point t_{fcz} are:

$$\begin{cases} t_{\text{fcz}} > \Delta t_{\text{prot}} + \Delta t_{\text{open}} + \Delta t_{\text{arcset}} \\ \hat{I}(t_{\text{fcz}} - \Delta t_{\text{arcset}}) < IR \end{cases} \quad (14)$$

Once t_{fcz} is determined, the delay Δt_{dl} can be calculated by:

$$\Delta t_{\text{dl}} = t_{\text{fcz}} - \Delta t_{\text{prot}} - \Delta t_{\text{open}} - \Delta t_{\text{arcset}} \quad (15)$$

Thus, the trip command should be delayed for Δt_{dl} from the protection operating instant. Comparing Fig. 1 and Fig. 2, it is noted that such a delay of tripping would not necessarily extend the fault clearing time if the arc could be extinguished at the same current zero-crossing as the conventional FDI mode, whereas the actual arcing time could be close to the minimum arcing time and the SCC excessive risk could be eliminated at contact separation.

3.3. Overall implementing process

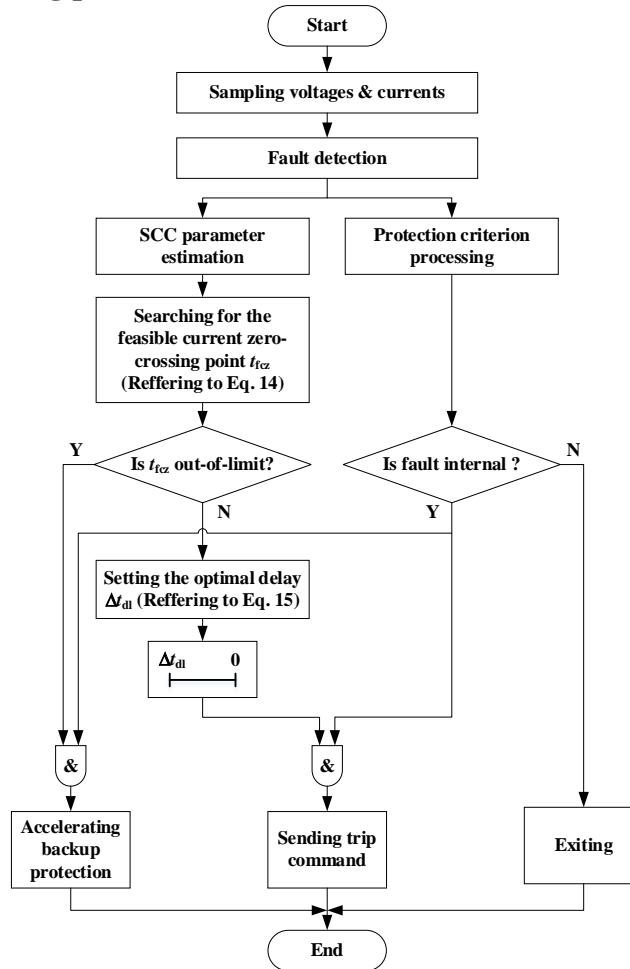


Fig. 3: Flowchart of the fault soft interruption scheme.

As illustrated in Fig. 3, the fault soft interruption scheme is supposed to collaborate with the protection system. The basic processing steps can be stated as below:

When a fault occurs, the fault detection algorithm would respond and determine the fault inception instant, triggering both the protection criterion judgment and the SCC estimation. The novel phaselet-based estimation method could produce the characteristic parameters of SCC within 1/4 cycle, faster than almost any protection algorithm so that no extra delay is led due to the heavy computation burden. If the protection identifies the fault as an internal one, unlike the conventional FDI mode sending the trip command directly, the proposed FSI scheme would search for the feasible current zero-crossing point t_{fcz} , and make a prospective delay Δt_{di} of the trip command to optimize the interrupting process of CB.

In case of no feasible current zero-crossing point existing in the critical fault clearing duration (mostly due to the dc time constant being extremely large), the delay should be set as zero instead of waiting blindly at the risk of endangering the system stability. One negative way is to turn into FDI mode, but the fault clearing time (FCT) could still be too long, ultimately responded by the backup protection. To improve that, based on the prediction results of FSI that the feasible current zero-crossing point would not be found, the associated backup protection could be accelerated, keeping the system as stable as possible. How to make the best choice between the above two options should be decided by experts according to the engineering situations.

4. Simulation Results

To verify the effectiveness of the proposed fault soft interruption scheme, a 500 kV, 50 Hz simplified equivalent power system is built in PSCAD with a sampling frequency of 4 kHz, as shown in Fig. 4, simulating the excessive SCC scenarios depicted in [15].

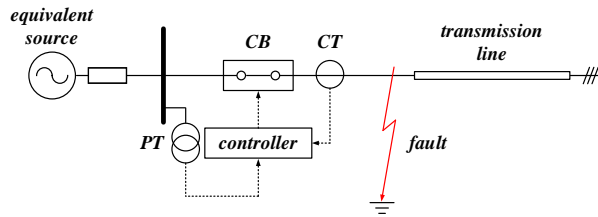


Fig. 4: Model of the 500 kV equivalent power system.

We choose a 500 kV, 63 kA CB as the research object, of which the rated symmetrical SCC interrupting capability $I_{sym} = 63 \text{ kA}$, i.e., the IR is 65.47 kA. Besides, the CB is set to be equipped with an intelligent control unit capable of phase controlled switching. At present, the software and hardware realization of such a unit and its effect on the operating characteristics of the CB have been fully studied [5-9]. Due to the space limitation, this paper would not repeat the previous work but concentrate on the viability of applying the principle of controlled switching technology to reduce the risk of interrupting excessive SCC.

Referring to the technical data provided by the manufacturer [23] and the investigation of the controlled switching performances [24], it is known that for the EHV CB, the rated opening time is 20 ms, and the reliable arcing time is above 9 ms, and the operating time dispersion can be limited within 1.5 ms. Thus, in the following cases, we assume: $\Delta t_{open} = 20 \text{ ms}$, $\Delta t_{arcmin} = 10 \text{ ms}$, and $\Delta t_{arcset} = 11.5 \text{ ms}$ (considering the safety-margin as 1.5 ms). In addition, for the sake of analysis, the corresponding protection is hypothesized to operate 10 ms after the fault inception, i.e., $\Delta t_{prot} = 10 \text{ ms}$.

4.1. Tripping process in a typical fault scenario

Letting a permanent three-phase fault occur at $t = 0 \text{ ms}$, of which the time constant $\tau = 60 \text{ ms}$, the fault inception angle (phase A) $\alpha_A = 0^\circ$, the current waveforms, and interrupting sequences of three phases are shown in Fig. 5. For the convenience of visualization, the waveforms of phase B, C are put opposite in sign to keep the so-called major loop (the half-wave with longer duration and larger magnitude) above the zero axis.

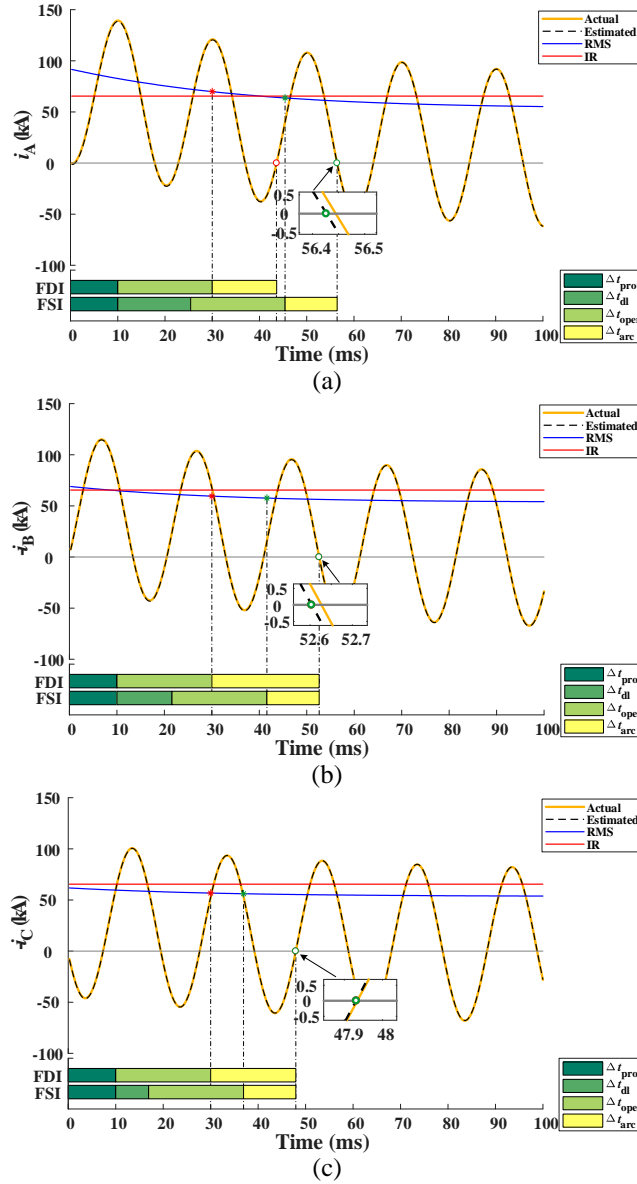


Fig. 5: Interruption of a typical three-phase fault. (a) Phase A; (b) Phase B; (c) Phase C.

Note that the dotted current waveforms are extrapolated by the proposed phaselet-based SCC estimation algorithm at $t = 5$ ms, ahead of the protection operating. Hence no extra calculating delay is made. It is apparent in Fig. 5 that such estimated SCC waveforms are rather close to the actual ones. Particularly, in any phase, the estimation errors of current zero-crossing points are no more than ± 0.1 ms, indicating the sufficient accuracy of the proposed estimation method.

In phase A, the RMS value of the ac symmetrical component is 53.55 kA, far less than the rated IR. However, the fault occurs at the voltage zero-crossing point ($\alpha_A = 0^\circ$), resulting in the greatest initial magnitude of the dc component. Under the conventional fault direct interruption mode (FDI), at the moment when the contacts of CB are about to part ($t = 30$ ms), the total RMS current remains 69.96 kA, exceeding the IR of the CB. Therefore, it is hazardous to trip the CB forcedly by the FDI. By comparison, according to the proposed FSI scheme, the trip command should be delayed from the protection operating instant ($\Delta t_{di} = 14.75$ ms), so that the RMS value of SCC at the desired contact parting moment decreases below the IR safely (63.69 kA), avoiding the SCC excessive risk.

In phase B and phase C, although there is no risk of SCC exceeding the IR, the FSI scheme is still superior to the FDI mode concerning shortening the arcing time. For example, by applying the FSI scheme, the arcing time of phase B is cut down from 22.75 ms (under FDI) to 11.50 ms.

4.2. Performance under different time constants

The decaying of the dc component depends on the time constant, which plays a key role in the occurrence of zero-crossing points and the magnitude of SCC.

Changing the X/R ratio of the equivalent system impedance, the performances of FSI and FDI are investigated under three-phase faults with a range of time constants ($\tau = 10 \sim 100$ ms). The simulation results related to phase A are presented in Fig. 6.

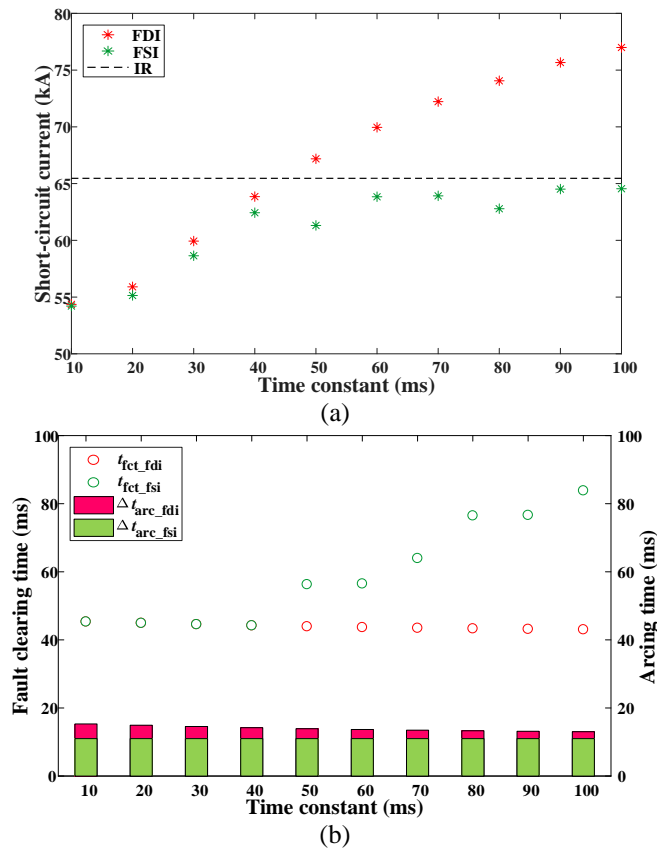


Fig. 6: Interruption under various time constants. (a) RMS value of SCC at contact separation; (b) Fault clearing time and arcing time.

Fig. 6 (a) shows that the total RMS value of SCC at the contact separation instant corresponding to FDI rises with the time constant. To be specific, the threats of SCC exceeding the IR are highlighted when $\tau > 50$ ms. In contrast with FDI attempting to trip the CB as soon as possible, FSI delays the trip command appropriately to secure the adequate decaying of SCC at the prospective instant, eradicating the SCC excessive risks no matter how large τ is.

Displayed as bar graphs in Fig. 6 (b), the arcing time can be minimized by FSI for any time constant, rather than appear randomly at a large level under the FDI mode. As for the fault clearing time, FSI can extinguish the arc at the same current zero-crossing point as FDI if $\tau < 40$ ms. For the larger time constant, FSI seems to extend the fault clearing time since a longer delay time is required to separate the contacts until the SCC decreases below IR. However, the fact is that in such severe fault scenarios, FDI may not trip the CB successfully due to the excessive SCC, leaving the fault lasting, similar to a breaker failure accident. As a result, it will take much longer to clear the fault by some backup protection, e.g., the breaker failure protection (10~12 cycles typically [16]). Therefore, the proposed FSI scheme can effectively circumvent the SCC excessive risks instead of being remedied by other time- and cost-consuming countermeasures after the failure of FDI.

4.3. Performance under different fault inception angles

Another essential factor is the fault inception angle, which can influence the proportion of the dc component as well. Taking phase A as an example, in the case of three-phase faults with a time constant of 60 ms, ranging α_A from 0° to 90° , the simulation results are shown in Fig. 7.

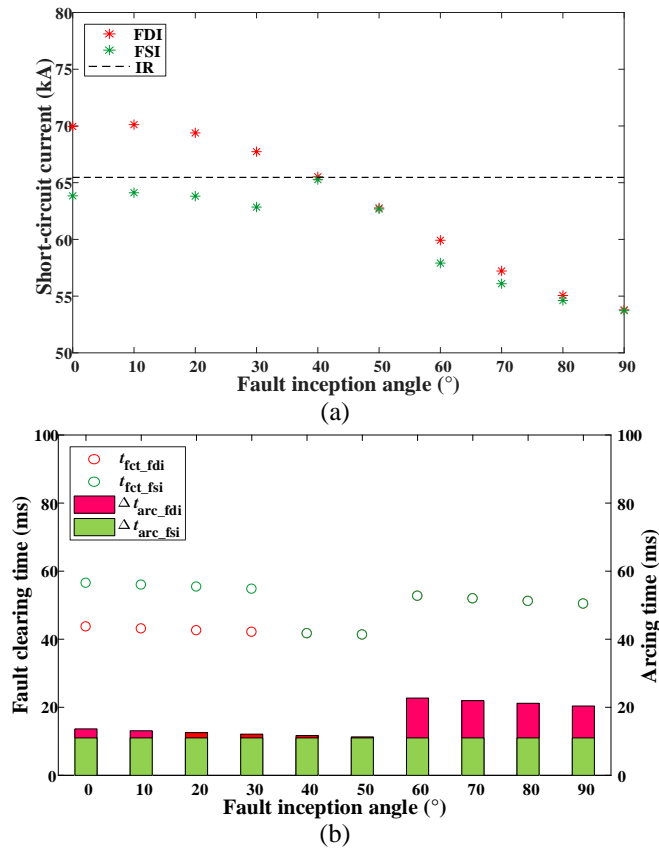


Fig. 7: Interruption under various fault inception angles. (a) RMS value of SCC at contact separation; (b) Fault clearing time and arcing time.

It can be seen from Fig. 7 that for $\alpha_A < 40^\circ$, FDI will trip the CB fiercely at the risk of SCC exceeding the IR, while for $\alpha_A > 50^\circ$, FDI will trip the CB through a longer arcing process, intensifying the contact erosion. By contrast, for any fault inception angle, FSI can cope with the potential SCC excessive risks while keeping the arcing time to the minimum degree, which is beneficial to maintaining the security of the CB and prolonging its life-cycle duration.

5. Conclusion

In the context of smart substations, the smart CB is becoming technologically and economically practical. To ease the fault clearing burden of the CB, a novel fault soft interruption scheme is proposed in this paper. The main results can be concluded as follows:

1) When the fault occurs exactly at the voltage zero-crossing point, the initial magnitude of the dc component can be up to the same value of the ac component. The larger the time constant is, the more highlighted SCC excessive risk at contact separation is. For the conventional mode, the CB is tripped blindly, leading to a potential interruption failure once SCC exceeds its rated capacity.

2) The proposed phaselet-based algorithm just requires a time window of less than 1/4 cycle, so it can complete the estimation before the protection operates. The simulation results confirm the reliability of such a method, by which the errors between the predicted current zero-crossing points and the actual ones are within ± 0.1 ms.

3) The determination of the feasible current zero-crossing point takes into account both the mitigation of SCC excessive risk and the minimization of arcing time. Thus, the electrical wear of CB can be reduced to a great extent, which is good for its life cycle. When coping with enormous SCC, the fault soft interruption scheme only delays the trip command appropriately, while the conventional way needs to be remedied by backup protection, which might lengthen the total fault clearing time and expand the fault scope.

6. Acknowledgements

This work was supported by the Science and Technology Project of State Grid Corporation of China (5100-202199545A-0-5-ZN).

7. References

- [1] Y. Liu, H. Gao, W. Gao and F. Peng. Development of a substation-area backup protective relay for smart substation. *IEEE Trans. Smart Grid*, 2017, 8(6): 2544-2553.
- [2] H. Wang, B. Zhou and X. Zhang. Research on the remote maintenance system architecture for the rapid development of smart substation in china. *IEEE Trans. Power Del.*, 2018, 33(4): 1845-1852.
- [3] A. Zheng, Q. Huang, D. Cai, et al.. Quantitative assessment of stochastic property of network-induced time delay in smart substation cyber communications. *IEEE Trans. Smart Grid*, 2020, 11(3): 2407-2416.
- [4] P. Li, X. Huang, J. Qi, H. Wei and X. Bai. A connectivity constrained MILP model for optimal transmission switching. *IEEE Trans. Power Syst.*, 2021, 36(5): 4820-4823.
- [5] J. Liu, G. M. Huang, Z. Ma and Y. Geng. A novel smart high-voltage circuit breaker for smart grid applications. *IEEE Trans. Smart Grid*, 2011, 2(2): 254-264.
- [6] B. Zhang, L. Ren, J. Ding, J. Wang, Z. Liu, Y. Geng and S. Yanabu. A relationship between minimum arcing interrupting capability and opening velocity of vacuum interrupters in short-circuit current interruption. *IEEE Trans. Power Del.*, 2018, 33(6): 2822-2828.
- [7] M. Chen, X. Duan, Z. Huang, J. Zou and E. Dong. Adaptive control for operating time of vacuum switch. *Proc. Chin. Soc. Electr. Eng.*, 2010, 30(36): 22-26.
- [8] X. Duan, M. Liao, J. Zou and Z. Huang. Fiber-controlled vacuum interrupter module used for fault current interruption. *Proc. 24th Int. Symp. Discharges Elect. Insul. Vacuum*, Braunschweig, 2010, pp. 166-169.
- [9] A. Poltl and K. Frohlich. A new algorithm enabling controlled short circuit interruption. *IEEE Trans. Power Del.*, 2003, 18(3): 802-808.
- [10] R. Thomas, J. Daalder and C. Sölver. An adaptive, self-checking algorithm for controlled fault interruption. *Proc. 18th Int. Conf. on Electr. Distrib.*, Turin, Italy, 2005, pp. 1-5.
- [11] X. Sun, M. Gao, D. Liu, X. Hou and R. Yuan. Analysis and processing of electrical fault signals with modified adaptive Prony method. *Proc. Chin. Soc. Electr. Eng.*, 2010, 30(28): 80-87.
- [12] J. Ding, S. Ai, W. Li, B. Zhang, X. Yao, Z. Liu, H. Zhang, C. Yang and X. Li. A fast current zeroes estimation algorithm for controlled fault interruption based on an improved BP neural network. *Proc. 4th Int. Conf. on Electr. Power Equipment*, China, 2017, pp. 924-928.
- [13] U. B. Parikh and B. R. Bhalja. SVR-based current zero estimation technique for controlled fault interruption in the series-compensated transmission line. *IEEE Trans. Power Del.*, 2013, 28(3): 1364-1372.
- [14] H. Li, A. Bose and Y. Zhang. On-line short-circuit current analysis and preventive control to extend equipment life. *IET Gener. Transm. Distrib.*, 2013, 7(1): 69-75.
- [15] W. Cao, Y. Wang, W. Zhang, X. Yang, X. Jin and B. Liu. Analysis on dc component in short-circuit current of power grid and its influence on breaking ability of circuit breakers. *Power Syst. Technol.*, 2012, 36(3): 283-288.
- [16] B. Kasztenny, V. Muthukrishnan and T. S. Sidhu. Enhanced numerical breaker failure protection. *IEEE Trans. Power Del.*, 2008, 23(4): 1838-1845.
- [17] Y. Xue, M. Thakhar, J. C. Theron and D. P. Erwin. Review of the breaker failure protection practices in utilities. *Proc. 65th Annu. Conf. Protect. Relay Eng.*, 2012, pp. 260-268.
- [18] L90 line current differential system [Online]. Available: <https://www.gegridsolutions.com>.
- [19] Z. Hao, J. Guan and W. Chen. Anti-saturation algorithm in differential protection based on the phaselet. *Proc. 5th Int. Conf. Electr. Utility Deregulation Restructuring Power Technol.*, Changsha, China, 2015, pp. 1030-1035.
- [20] IEC standard for high-voltage switchgear and controlgear - part 100: alternating-current circuit-breakers, IEC 62271-100, Sep. 2012.
- [21] IEEE application guide for ac high-voltage circuit breakers > 1000 V ac rated on a symmetrical current basis, IEEE Std C37.010-2016, Apr. 2017.

- [22] IEEE standard for ac high-voltage circuit breakers rated on a symmetrical current basis - preferred ratings and related required capabilities for voltages above 1000 V, IEEE Std C37.06-2009, Nov. 2009.
- [23] Live tank circuit breakers (72.5-550 kV) [Online]. Available: <https://www.gegridsolutions.com>.
- [24] T. Kobayashi, S. Tsukao, I. Ohno, T. Koshizuka, S. Nishiwaki, N. Miyake, K. Matsushita, and T. Saida. Application of controlled switching to 500-kV shunt reactor current interruption. *IEEE Trans. Power Del.*, 2003, 18(2): 480-486.